AJNR

Kimura Disease: CT and MR Imaging Findings

S.-W. Park, H.-J. Kim, K.J. Sung, J.H. Lee and I.S. Park

AJNR Am J Neuroradiol 2012, 33 (4) 784-788
doi: https://doi.org/10.3174/ajnr.A2854
http://www.ajnr.org/content/33/4/784

ORIGINAL RESEARCH

Kimura Disease: CT and MR Imaging Findings

S.-W. Park
H.-J. Kim
K.J. Sung
J.H. Lee
I.S. Park

BACKGROUND AND PURPOSE: KD is a rare chronic inflammatory disorder of unknown etiology. The purpose of this study was to evaluate the CT and MR imaging findings of KD in the head and neck.

MATERIALS AND METHODS: We retrospectively reviewed the CT (n = 21) and MR (n = 9) images obtained in 28 patients (24 males and 4 females; mean age, 32 years; age range, 10–62 years) with histologically proved KD in the head and neck.

RESULTS: In these 28 patients, CT and MR images demonstrated a total of 52 non-nodal lesions, 1–8 cm in greatest diameter, in the head and neck. The lesions were unilateral in 11 patients and bilateral in 17 patients. Eleven patients had a solitary lesion, and 17 patients had 2–4 lesions. The parotid and/or periparotid area was the most frequent location, with 36 lesions in 23 patients. The margin of the lesions was well-defined in 1 and ill-defined in 51 cases. Compared with the adjacent muscle, the MR signal intensity of all lesions was iso- to slightly hyperintense on T1-weighted images and hyperintense on T2-weighted images. Most of the lesions demonstrated mild or moderate enhancement on postcontrast CT scans and moderate or marked enhancement on postcontrast MR images. MR images also showed tubular signal-intensity voids in 7 of 13 lesions. Associated lymphadenopathy was demonstrated in 23 patients, usually bilaterally.

CONCLUSIONS: Multiple ill-defined enhancing masses within and around the parotid gland with associated regional lymphadenopathy are characteristic CT and MR imaging findings of KD in the head and neck.

ABBREVIATIONS: ALHE = angiolymphoid hyperplasia with eosinophilia; IgE = immunoglobulin E; KD = Kimura disease

KD is a rare chronic inflammatory disorder of unknown etiology, characterized by angiolymphoid proliferation with peripheral eosinophilia and elevated serum IgE. The disease has a predilection for the head and neck and typically occurs in young Asian males.[1,2] Although it was first described in the Chinese literature in 1937 under the designation of "eosinophilic hyperplastic lymphogranuloma," it was not until 1948 that the disease to become widely known as KD when Kimura and Ishikawa[3] reported it in the Japanese literature.[4] KD often produces subcutaneous tumorlike nodules with frequently associated involvement of the major salivary gland and regional lymph nodes.[5]

Although the clinical and histopathologic findings of KD have been well described in the literature, only a few reports have dealt with its radiologic findings, and generally as case reports or small case series.[6-15] The purpose of this study was to describe the CT and MR imaging findings of histologically proved KD involving the head and neck in 28 patients. To our knowledge, this is the largest imaging study of patients with KD of the head and neck.

Received May 22, 2011; accepted after revision July 27.

From the Department of Radiology (S.-W.P.), Boramae Medical Center, Seoul National University College of Medicine, Seoul, Korea; Department of Radiology (S.-W.P.), Inha University Hospital, Incheon, Korea; Department of Radiology (H.-J.K.), Samsung Medical Center, Sungkyunkwan University School of Medicine, Seoul, Korea; Department of Radiology (K.J.S.), Wonju Christian Hospital, Yonsei University Wonju College of Medicine, Wonju, Korea; Department of Radiology and Research Institute of Radiology (J.H.L.), Asan Medical Center, University of Ulsan College of Medicine, Seoul, Korea; and Department of Pathology (I.S.P.), Inha University College of Medicine, Incheon, Korea.

Please address correspondence to Hyung-Jin Kim, MD, Department of Radiology, Samsung Medical Center, Sungkyunkwan University School of Medicine, 50 Ilwon-dong, Gangnam-gu, Seoul 135-710, Korea; e-mail: hyungkim@skku.edu

http://dx.doi.org/10.3174/ajnr.A2854

Materials and Methods

Patients

This study was approved by our institutional review board, and informed consent was waived in accordance with the requirements of a retrospective study. We reviewed CT (n = 21) and MR (n = 9) images obtained from 28 patients with histologically proved KD of the head and neck. The patients were identified by a search of the electronic data base and the pathology registry from 4 tertiary academic hospitals during the past 7 years. There were 24 men (86%) and 4 women (14%), 10–62 years of age, with a mean age of 32 years. Nineteen patients (68%) were in their second-to-fourth decades. All patients presented with painless masses or swelling in the head and neck with a duration of 2 months to 25 years (mean, 7.6 years). In all patients, the diagnosis was confirmed by excisional biopsy, including biopsy of multiple lesions in 8 of 17 patients who had multiple lesions in the head and neck. Two patients had an additional mass in the upper extremity, which also proved to be KD histologically.

All patients had eosinophilia in the peripheral blood, ranging from 12.1% to 55.5% (mean, 28.5% [normal range, 5%]). The serum IgE level, which was checked in 9 patients, was elevated >1000 IU/mL (normal range, ≤378 IU/mL) in all patients. No patients had associated renal disease.

Imaging Techniques

CT was performed in 21 patients, and MR imaging, in 9 patients. Two patients underwent both CT and MR imaging examinations. CT scans were obtained in the axial plane 40–90 seconds after the intravenous administration of 60–100 mL of iodinated contrast material at a rate of 3 mL/s by using various models of a helical CT scanner with 2.5- to 3.75-mm section thicknesses. Precontrast CT scans were also available in 12 patients. MR imaging examinations were performed on a 1.5T (n = 8) or a 3T (n = 1) scanner to produce pre- and

postcontrast T1-weighted spin-echo images and T2-weighted fast spin-echo images with or without fat saturation. Postcontrast MR images were obtained 4 minutes after the intravenous injection of 0.1 mmol/kg of gadopentetate dimeglumine. Images were obtained in at least 2 planes with 3- to 5-mm section thickness and 0.3- to 1-mm intersection gap.

Image Analysis

Two experienced head and neck radiologists (with clinical experience of 21 and 12 years) retrospectively reviewed CT and MR images for the location (including multiplicity and bilaterality), size, margin, CT attenuation, MR signal-intensity characteristics, and pattern and degree of enhancement of the non-nodal lesions. We considered the lesions non-nodal if their location was not typical of cervical lymph nodes and/or if their shape was irregular or lobulated rather than round, oval, or bean-shaped. The size of the lesion was measured at its greatest diameter. The margin of the lesion was classified as well-defined and ill-defined. We compared the attenuation of the lesion on precontrast CT scans with that of the adjacent muscle. The presence of any calcification within the lesion determined on precontrast CT scans was also recorded. The signal intensity of the lesion on T1- and T2-weighted MR images was also compared with that of the adjacent muscle. On postcontrast CT and MR images, the pattern of enhancement of the lesion was categorized as homogeneous or heterogeneous. The degree of enhancement was graded by considering enhancement similar to that in the adjacent muscle as being mild; greater than the muscle but less than the sinonasal mucosa, moderate; and marked, similar to or greater than the sinonasal mucosa. As for the enhancement degree on MR images, we relied on first-phase postcontrast images in all patients.

We also investigated the presence of associated lymphadenopathy. Lymph nodes were considered abnormal if enhancement greater than that in the adjacent muscle was seen on postcontrast CT and MR images in nodes with long-axis diameter >10 mm. Discrepancies, if any, were resolved by consensus.

Summary of CT and MR imaging characteristics of non-nodal KD lesions of the head and neck

Imaging Characteristics	No. of Lesions
Location (n = 52)	
Parotid/periparotid	36
Parotid + periparotid	23
Parotid only	4
Periparotid only	9
Buccal space	6
Lacrimal gland	4
Submandibular/submental	3
Scalp	3
Margin (n = 52)	
Well-defined	1
Ill-defined	51
Density on precontrast CT scans (n = 22)[a]	
Hypodense	4
Isodense	18
Signal intensity on MR images (n = 13)[a]	
T1-weighted images	
Isointense	11
Hyperintense	2
T2-weighted images	
Hyperintense	13
Enhancement on postcontrast CT scans (n = 43)	
Homogeneous	
Mild	10
Moderate	22
Marked	3
Heterogeneous	
Mild	2
Moderate	6
Enhancement on postcontrast MR images (n = 13)	
Homogeneous	
Moderate	2
Marked	10
Heterogeneous, marked	1

[a] Density and signal intensity of the lesion were compared with those of the adjacent muscle.

Results

In 28 patients, CT and MR images demonstrated a total of 52 non-nodal lesions in the head and neck. The lesions were unilateral in 11 patients and bilateral in 17 patients. Eleven patients (39%) had a solitary lesion, and 17 patients (61%) had ≥2 lesions (2 lesions in 13 patients, 3 lesions in 1 patient, and 4 lesions in 3 patients).

The CT and MR imaging features of the 52 non-nodal lesions are summarized in the Table. The parotid and/or periparotid area (including pre- and postauricular areas) was the most frequent location involved in 36 (69%) of 52 lesions in 23 (82%) of 28 patients, either unilaterally (13 patients) or bilaterally (10 patients) (Figs 1 and 2). Of these 36 lesions, the parotid gland was involved in 27 lesions, either solely (n = 4) or concomitantly with the periparotid soft tissue (n = 23). Other locations less commonly involved were the buccal area (6 lesions in 5 patients, Fig 3), lacrimal gland (4 lesions in 2 patients, Fig 4), submandibular/submental area (3 lesions in 2 patients), and scalp (3 lesions in 2 patients, Fig 2*A*). The size of the lesions ranged from 1 to 8 cm in greatest diameter with a mean of 4.1 cm. The margin of the lesions was well-defined in 1 (2%) and ill-defined in 51 (98%).

Precontrast CT scans obtained in 12 patients demonstrated a total of 22 non-nodal lesions. Compared with the adjacent muscle, the attenuation of the lesion was isoattenuated in 18 and hypoattenuated in 4. No lesion contained calcification demonstrable on CT scans. Compared with the adjacent muscle, the signal intensity of 13 non-nodal lesions assessed on MR imaging in 9 patients was iso- (n = 11) or slight hyperintensity (n = 2) on T1-weighted images. All lesions were seen as hyperintense masses on T2-weighted images (Figs 1 and 2). Postcontrast CT scans obtained in 21 patients demonstrated a total of 43 non-nodal lesions. Mild (n = 10), moderate (n = 22), or marked (n = 3) homogeneous enhancement was seen in 35 lesions (Fig 2). The remaining 8 lesions showed heterogeneous enhancement, either mild (n = 2) or moderate (n = 6). Thirteen lesions detected by postcontrast T1-weighted MR images showed moderate (n = 2) or marked (n = 10) homogeneous enhancement in 12 and marked heterogeneous enhancement in 1 (Figs 1, 3, and 4). Seven lesions in 5 patients contained tubular signal-intensity voids on T2-weighted and postcontrast T1-weighted MR images, probably representing fast-flowing vascular structures (Figs 1*C* and 3*B*). Associated lymphadenopathy was demonstrated in 23 (82%) of 28 patients (Fig 2) and was more common bilaterally (n = 16) than unilaterally (n = 7).

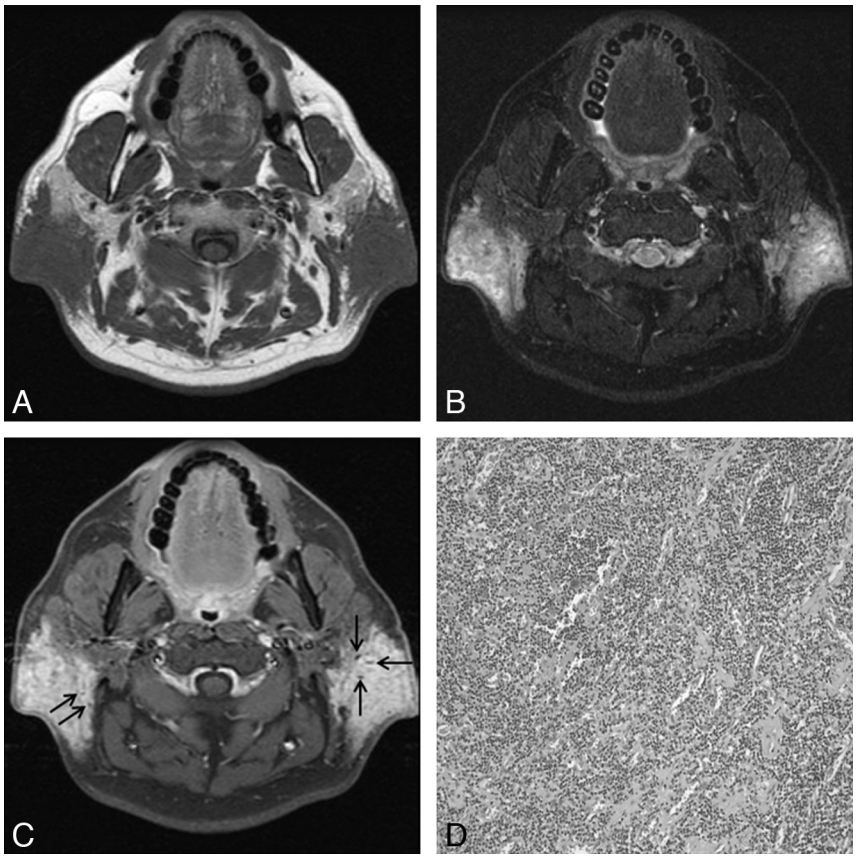

Fig 1. KD involving bilateral parotid and periparotid areas in a 45-year-old man. *A* and *B*, Axial MR images show ill-defined soft-tissue masses in the bilateral retroauricular areas with infiltration of the adjacent parotid gland. Compared with the adjacent muscle, the lesions are isointense on the T1-weighted image (*A*) and hyperintense on the fat-suppressed T2-weighted image (*B*). *C*, Postcontrast fat-suppressed T1-weighted image shows homogeneous marked enhancement. Note multiple dotlike signal-intensity voids within the lesions, probably representing vascular structures (*arrows* in *C*). *D*, Photomicrograph shows attenuated lymphoid infiltrates rich in eosinophils surrounding numerous thin-walled vascular structures (hematoxylin-eosin, original magnification ×100).

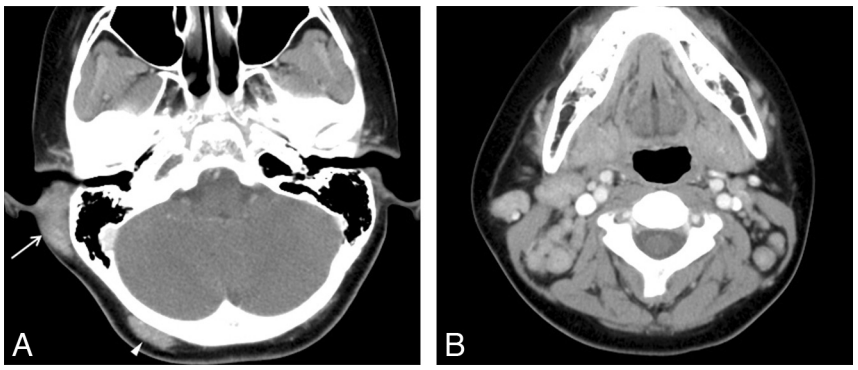

Fig 2. KD involving the postauricular area and occipital scalp in an 11-year-old boy. *A*, Postcontrast axial CT scan shows an ill-defined soft-tissue mass with homogeneous moderate enhancement involving the postauricular area on the right (*arrow*). Also note a smaller mass with the similar imaging characteristics on the right occipital scalp (*arrowhead*). *B*, Postcontrast axial CT scan shows multiple moderately enhancing and enlarged lymph nodes, right greater than left, on both sides of the neck.

Discussion

KD is a chronic inflammatory disease characterized histologically by proliferation of folliculoid structures, which are infiltrated by eosinophils, plasma cells, lymphocytes, and mast cells and demonstrate associated vascular proliferation and stromal fibrosis.[9] Fibrosis can be present in the early stage of the lesions and may be replaced later by hyalinization.[4,13] Many synonymous terms have been used to describe KD, including subcutaneous eosinophilic lymphoid granuloma, eosinophilic lymphoid follicular hyperplasia, and eosinophilic folliculosis of the skin.[5,14,15] Although the cause of KD still remains unknown, it may be a self-limited allergic or autoimmune response to an unknown stimulus; this hypothesis is supported by the increased eosinophil count and IgE in the peripheral blood.[13,15] It has been speculated that a viral or parasitic trigger may alter T-cell immunoregulation or induce an IgE-mediated type 1 hypersensitivity, resulting in the release of eosinophilotrophic cytokines.[13,16]

Clinically, KD primarily affects those of Asian descent in their second, third, and fourth decades of life with a male

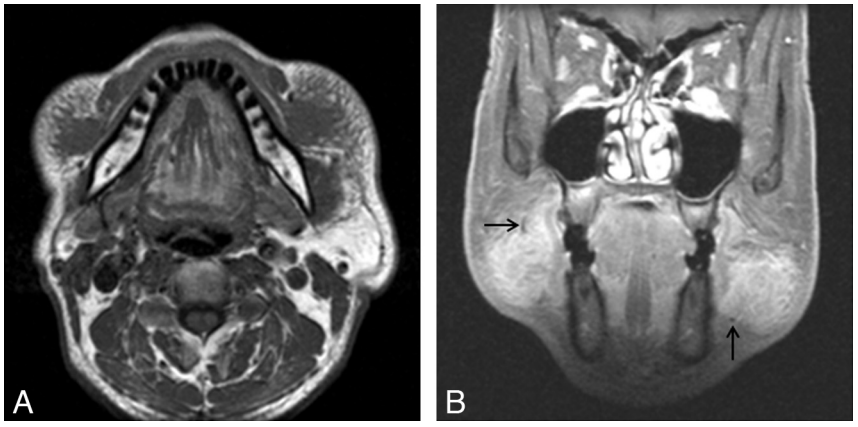

Fig 3. KD involving bilateral buccal spaces in a 52-year-old man. *A,* Axial T1-weighted MR image demonstrates ill-defined soft-tissue masses in the bilateral buccal spaces, isointense to the adjacent muscle. Note the reticular infiltration of the subcutaneous tissue around the lesions. *B,* Postcontrast coronal fat-suppressed T1-weighted MR image demonstrates homogeneous marked enhancement of the lesions. Note tubular or dotlike signal-intensity voids at the periphery of the lesions, probably representing fast-flowing vascular structures (*arrows*).

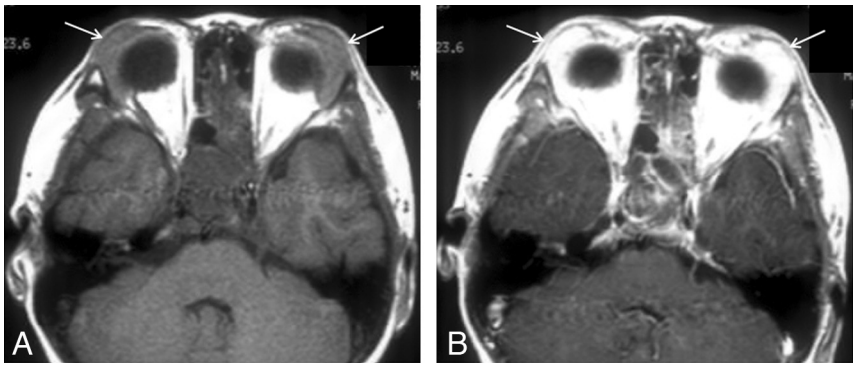

Fig 4. KD involving bilateral lacrimal glands in a 13-year-old boy. *A,* Axial T1-weighted MR image shows diffuse enlargement of bilateral lacrimal glands (*arrows*). The signal intensity of the lesions is slightly hyperintense to the adjacent muscle. *B,* Postcontrast axial T1-weighted MR image shows homogeneous marked enhancement of the lesions (*arrows*).

predilection (87%).[6,9,15] Most patients present with firm, painless, single, or multiple subcutaneous lesions in the head and neck, especially in the parotid and submandibular regions.[2,13] Associated lymphadenopathy is frequent, with a reported incidence of 42%–100%.[15] Less common sites of involvement in the head and neck include the paranasal sinuses, orbits (including eyelids, conjunctiva, and lacrimal glands), epiglottis, tympanic membrane, and parapharyngeal space.[17] Rarely the disease can involve non-head and neck sites such as the axilla, groin, popliteal region, and forearm.[2,18] Although the clinical course of KD is typically progressive for several years, the disease is generally benign and self-limited, though it may be complicated by renal involvement, notably nephrotic syndrome.[10] Characteristically, there is accompanying peripheral blood eosinophilia (10%–70%) and an elevated serum IgE level (800–35,000 IU/mL),[2,9] which may fluctuate in the course of the disease. Several studies reported a close relationship between the lesion size and the degree of eosinophilia—that is, the bigger the lesion, the greater the eosinophilia in peripheral blood.[19,20] Serum concentrations of eosinophil cationic protein might be used as an additional parameter of disease activity.[19,21]

The results of the present study are generally in accordance with those of previous studies: male predilection (86%), age distribution (mean age, 32 years; 68% occurring in the second-to-fourth decades), multiplicity (61%), parotid/peripa-rotid predilection (69% of lesions seen in 82% of patients), and lymphadenopathy (82%). In contrast with the previous studies, our patients had bilateral disease (61%) more commonly than unilateral disease.

The diagnosis of KD may be difficult because clinicians and pathologists in Western countries are relatively unfamiliar with this rare disease, and unnecessary diagnostic tests and procedures are frequently performed to exclude other serious disorders such as tumors. In this context, although pathologic confirmation is necessary for the definite diagnosis of KD, imaging studies including CT and MR imaging can be useful for suggesting a specific diagnosis as well as delineating the extent of the disease. There have been several reports suggesting that the radiologic findings of KD of the head and neck are nonspecific and variable.[6-15] On CT scans, either well-defined nodular masses or ill-defined plaquelike infiltrative masses in the subcutaneous tissue associated with lymphadenopathy are reported as the typical findings.[7,15] Most of the lesions are seen in the vicinity of the major salivary glands, especially the parotid gland.[15] The attenuation of the masses varies from iso- to hyperattenuated.[12,14] On MR images, the masses are reported to show variable signal intensity—that is, low-to-high signal intensity on T1- and T2- weighted images.[7,9,12-14] On postcontrast CT and MR imaging, enhancement patterns vary from mild to intense and from homogeneous to heterogeneous.[7,9,13,14] Sometimes, MR images demonstrate serpentine

signal-intensity-void areas, suggestive of vascular structures, within the lesions, as seen in 7 of 13 lesions in the present study. In the study on MR imaging findings of 9 cases of KD involving the upper extremity, Choi et al[18] reported dotlike or tubular signal-intensity voids within the mass in all 9 cases. In the head and neck, a similar finding was described once before.[7]

The variability in the degree of enhancement on CT and MR images and the signal intensity on MR images are thought to be attributed to the different degrees of fibrosis and vascular proliferation contained in the individual lesions.[9,12,18] Abundant vascular proliferation may explain the presence of enhancement and signal-intensity-void structures on MR images.[18] In the present study, most of the lesions (98%) showed ill-defined borders on CT and MR images. Compared with that in the adjacent muscle, the signal intensity of the lesions was iso- to slightly hyperintense on T1-weighted images and hyperintense on T2-weighted images. The degree of enhancement of the lesions was generally greater on postcontrast MR images than on postcontrast CT scans, reflecting the higher sensitivity of MR imaging to detect changes after contrast enhancement. Eleven of 13 lesions detected on postcontrast MR images showed marked contrast enhancement, which was noted in only 3 of 43 lesions on postcontrast CT scans. The observed difference in enhancement between CT and MR imaging may also be attributed to the different timing of these imaging studies. While postcontrast CT scans of the neck are usually acquired with a relatively short delay after contrast injection, postcontrast MR images take longer to acquire, reflecting the pattern of enhancement in which there is delayed wash-in and slow washout.

The imaging differential diagnosis for KD in the head and neck includes parotid tumors, lymphoma, metastatic tumors, malignant tumors of cutaneous or subcutaneous origin, tuberculosis, and ALHE.[9,12,14,15] The parotid tumors are usually encapsulated or pseudoencapsulated and are limited to the parotid gland, while KD is frequently associated with irregular extension into the subcutaneous tissue. Although lymphoma and metastatic lymphadenopathy may have similar presentations, the irregular margination of the lesions and the distribution of the lesions, as well as the long clinical course as seen in KD, are unusual.[12,15] Enhanced lymphadenopathy associated with tuberculosis usually demonstrates central hypoattenuation and peripheral rim enhancement, whereas enlarged lymph nodes enhance homogeneously in KD.[9] KD can be confused clinically and histologically with ALHE, also known as epitheloid hemangioma, which is a rare but distinctive vascular tumor typically occurring in women.[16] ALHE, however, usually presents as small erythematous dermal nodules in the head and neck that itch and bleed easily. There is less common association with lymphadenopathy and peripheral eosinophilia. Histologically, fibrosis is lacking in ALHE, whereas it is prominent at all stages in KD.[15] Other entities that may present similarly to KD include posttransplant lymphoproliferative disorder, pseudotumor, Kuttner tumor, Castleman disease, and Sjogren syndrome.

The treatment of KD is not well-established. Although surgical excision is the preferred method of initial treatment, recurrence is common.[7,12,16,19,20] Other therapeutic options include radiation therapy, systemic corticosteroids, cytotoxic agents, cyclosporin, and pentoxifylline, with variable responses.[16,19,20] The recurrence rate is lower when ≥2 therapies are combined.[12]

Conclusions

KD is an uncommon, chronic, usually self-limited, inflammatory disease that should be differentiated from malignant tumors. Multiple ill-defined and at least moderately enhancing masses within and around the parotid gland with associated regional lymphadenopathy are the characteristic CT and MR imaging findings of KD in the head and neck.

References

1. Kuo TT, Shih LY, Chan HL. **Kimura's disease: involvement of regional lymph nodes and distinction from angiolymphoid hyperplasia with eosinophilia.** *Am J Surg Pathol* 1988;12:843–54
2. Chen H, Thomson LD, Aguilera NS, et al. **Kimura disease: a clinopathologic study of 21 cases.** *Am J Surg Pathol* 2004;28:505–13
3. Kimura T, Yoshimura S, Ishikawa E. **Unusual granulation combined with hyperplastic changes of lymphatic tissue** [in Japanese]. *Trans Soc Pathol Jpn* 1948;37:179–80
4. Kung IT, Gibson JB, Bannatyne PM. **Kimura's disease: a clinicopathological study of 21 cases and its distinction from angiolymphoid hyperplasia with eosinophilia.** *Pathology* 1984;16:39–44
5. Li TJ, Chen XM, Wang S-Z, et al. **Kimura's disease: a clinicopathologic study of 54 Chinese patients.** *Oral Surg Oral Med Oral Pathol Oral Radiol Endod* 1996; 82:549–55
6. Smith JR, Hadgis C, Van Hasselt A, et al. **CT of Kimura disease.** *AJNR Am J Neuroradiol* 1989;10(5 suppl):S34–36
7. Som PM, Biller HF. **Kimura disease involving parotid gland and cervical nodes: CT and MR findings.** *J Comput Assist Tomogr* 1992;16:320–22
8. Ahuja AT, Loke TK, Mok CO, et al. **Ultrasound of Kimura's disease.** *Clin Radiol* 1995;50:170–73
9. Takahashi S, Ueda J, Furukawa T, et al. **Kimura disease: CT and MR findings.** *AJNR Am J Neuroradiol* 1996;17:382–85
10. Goldenberg DGA, Barki Y, Leiberman A, et al. **Computerized tomographic and ultrasonographic features of Kimura's disease.** *J Laryngol Otol* 1997;111: 389–91
11. Ginsberg LE, McBride JA. **Kimura's disease.** *AJR Am J Roentgenol* 1998;171: 1508
12. Hiwatashi A, Hasuo K, Shiina T, et al. **Kimura's disease with bilateral auricular masses.** *AJNR Am J Neuroradiol* 1999;20:1976–78
13. Oguz KK, Ozturk A, Cila A. **Magnetic resonance imaging findings in Kimura's disease.** *Neuroradiology* 2004;46:855–58
14. Takeish M, Makino Y, Nishioka H, et al. **Kimura disease: diagnostic imaging findings and surgical treatment.** *J Craniofac Surg* 2007;18:1062–67
15. Gopinathan A, Tan TY. **Kimura's disease: imaging patterns on computed tomography.** *Clin Radiology* 2009;64:949–99
16. Shetty AK, Beaty MW, McGuirt WF, et al. **Kimura's disease: a diagnostic challenge.** *Pediatrics* 2002;110:e39
17. Keng CG, Pang KP, Teng PW. **Kimura's disease of the parapharyngeal space.** *Ear Nose Throat J* 2006;85:106–08
18. Choi J-A, Lee G-K, Kong KY, et al. **Imaging findings of Kimura's disease in the soft tissue of the upper extremity.** *AJR Am J Roentgenol* 2005;184:193–99
19. Sun QF, Xu DZ, Pan SH, et. al. **Kimura disease: review of the literature.** *Int Med J* 2008;38:668–72
20. Masayuki S, Ayako K, Shinichi N. **Hematoserological analysis of Kimura's disease for optimal treatment.** *Otolaryngol Head Neck Surg* 2005;132:159–60
21. Ohta N, Okazaki S, Fukase S, et al. **Serum concentrations of eosinophil cationic protein and eosinophils of patients with Kimura's disease.** *Allergol Int* 2007; 56:45–49